

Slope Turbulence, Internal Waves and Phytoplankton Growth at the Celtic Sea Shelf-Break [and Discussion]

R. D. Pingree, G. T. Mardell and D. E. Cartwright

Phil. Trans. R. Soc. Lond. A 1981 **302**, 663-682
doi: 10.1098/rsta.1981.0191

References

Article cited in:

<http://rsta.royalsocietypublishing.org/content/302/1472/663#related-urls>

Email alerting service

Receive free email alerts when new articles cite this article - sign up in the box at the top right-hand corner of the article or click [here](#)

To subscribe to *Phil. Trans. R. Soc. Lond. A* go to: <http://rsta.royalsocietypublishing.org/subscriptions>

Slope turbulence, internal waves and phytoplankton growth at the Celtic Sea shelf-break

BY R. D. PINGREE† AND G. T. MARDELL†

Institute of Oceanographic Sciences, Wormley, Godalming, Surrey GU8 5UB, U.K.

[Plates 1 and 2]

The edge of the Celtic Sea shelf is characterized during the summer by a band of cold water (*ca.* 100 km broad), which is generally conspicuous in high resolution infrared images from satellites, particularly under high pressure atmospheric conditions with clear skies. Preliminary studies of mixing in this region were made in 1972, 1973 and 1974 and were followed by more detailed interdisciplinary studies in 1976, 1979 and 1980 relating phytoplankton growth to the ways in which turbulence in the environment controls the availability of nutrients and light energy. The results have shown the cooler water to be about 1–2 °C colder than the adjacent surface waters of the Celtic Sea and Atlantic Ocean. This cold band also exhibits higher than background surface values of inorganic nitrate and chlorophyll *a*. Although these values are generally low compared with the values that have been observed near the neighbouring shelf tidal fronts, the increased surface values along the shelf break in summer appear to be significant. The observed increases of chlorophyll *a* are thought to be related to physical processes associated with the slopes, ridges and canyons where enhanced mixing, particularly due to internal waves or upwelling, results in nutrient renewal and subsequent phytoplankton growth along the shelf-break region of the Celtic Sea.

INTRODUCTION

The edge of the Celtic Sea shelf and the Armorican continental shelf to the south exhibit topographic changes from 200 m to 4000 m within an average horizontal distance of 60 km. This steep slope is also indented with many major canyons and ridges normal to its axis (Laughton 1975). During preliminary oceanographic surveys of the Celtic Sea slope in the summers of 1972 and 1973 it was found that the surface waters over the slope were colder than the adjacent surface waters of the Celtic Sea and Atlantic Ocean. This colder band (shelf-break front) was subsequently highlighted with the advent of high resolution infrared imagery (figure 1*b*, plate 1) which showed that on occasions the cooler band followed the shelf break for up to 800 km north of latitude 46° N. During the summers of 1976, 1979 and 1980 continuous surface and profiling measurements of sea temperature, salinity, chlorophyll *a* and inorganic nutrients were made at portions of the shelf break (figure 1*a*) by using STDs and pumping systems, XBTs, fluorometers, nutrient analysers and a towed undulating CTD (batfish) with an *in situ* fluorometer. These measurements and results from current meter moorings have been used in conjunction with many satellite infrared images of the area, from NOAA-5, NOAA-6 and TIROS-N, and some synthetic aperture radar results from SEASAT, to examine slope mixing processes and their effects on phytoplankton distributions along the slope region of the Celtic Sea.

† Present address: Marine Biological Association of the United Kingdom, The Laboratory, Citadel Hill, Plymouth PL1 2PB, U.K.

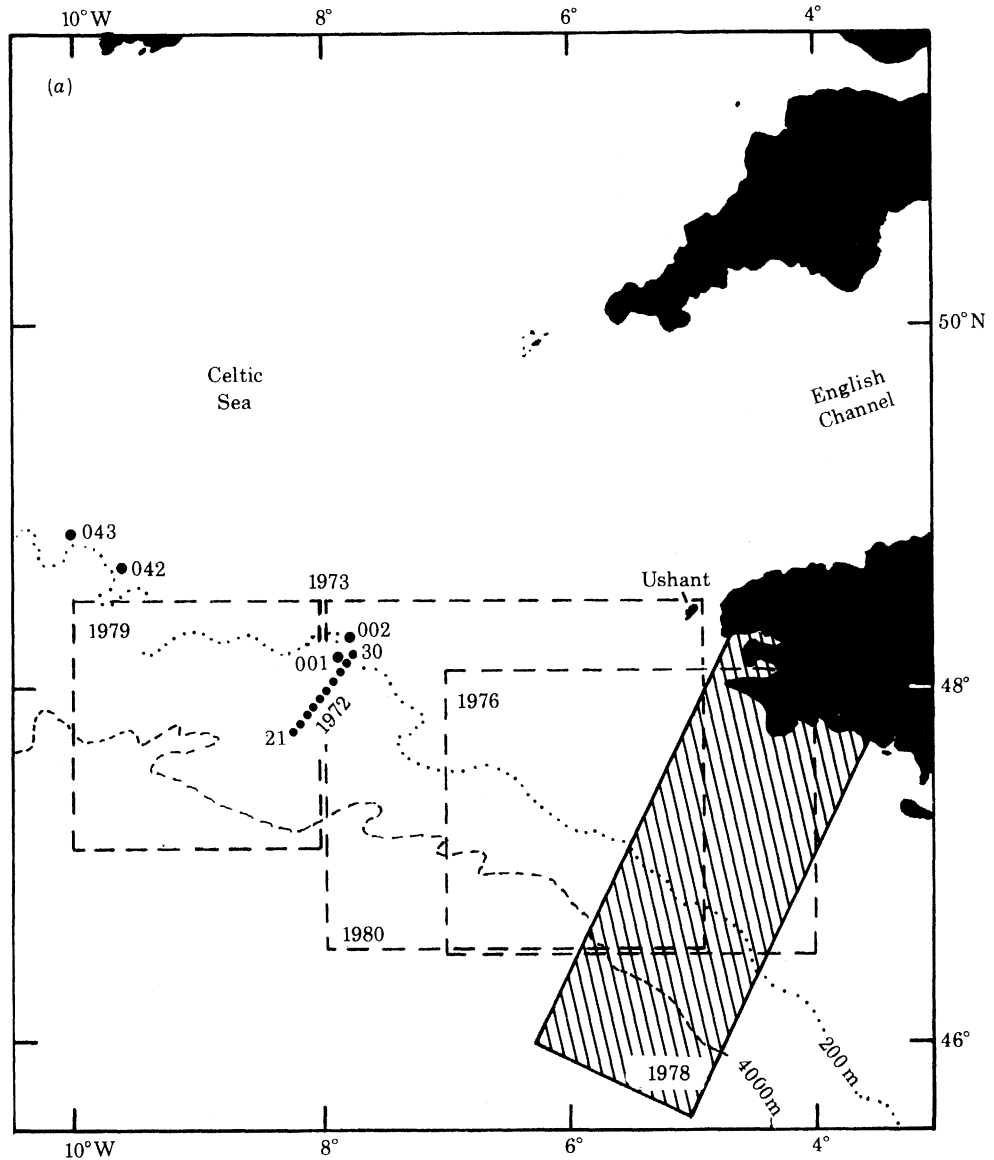


FIGURE 1(a). For description, see plate 1.

OBSERVATIONS

(a) *At sea*

In June 1972 STD sections were completed across the shelf (figures 1 *a*, 2 *a*, *b*, *c*) with measurements to within 2 m of the bottom in water depths less than 800 m. Although the surface temperatures are low compared with those later in the summer, they exhibit the same gross features seen as typical in later years. The most obvious feature is that the seasonal thermocline at the shelf break is broader in vertical extent than the adjacent oceanic and shelf waters. The shelf-water near the shelf break is characterized by an extensive (greater than 100 m) isothermal bottom layer (Pingree & Griffiths 1974) due to tidal mixing, which results in a restricted region for thermocline development between the wind-mixed layer and the bottom-mixed layer.



FIGURE 1. (a) Areas of detailed surveys on R.V. *Sarsia* in 1973, 1976, 1979 and 1980. The line of dots represents a series of STD stations completed in 1972. The shaded area represents the area covered by the synthetic aperture radar (s.a.r.) pass from SEASAT (see figure 9). The positions of shelf-break current meter moorings 001, 002 (see text and figure 13), 042, and 043 are also indicated. (b) Infrared image taken from NOAA-6 on 19th June 1979, showing cooling at the shelf break and the Ushant front. White represents low temperatures.

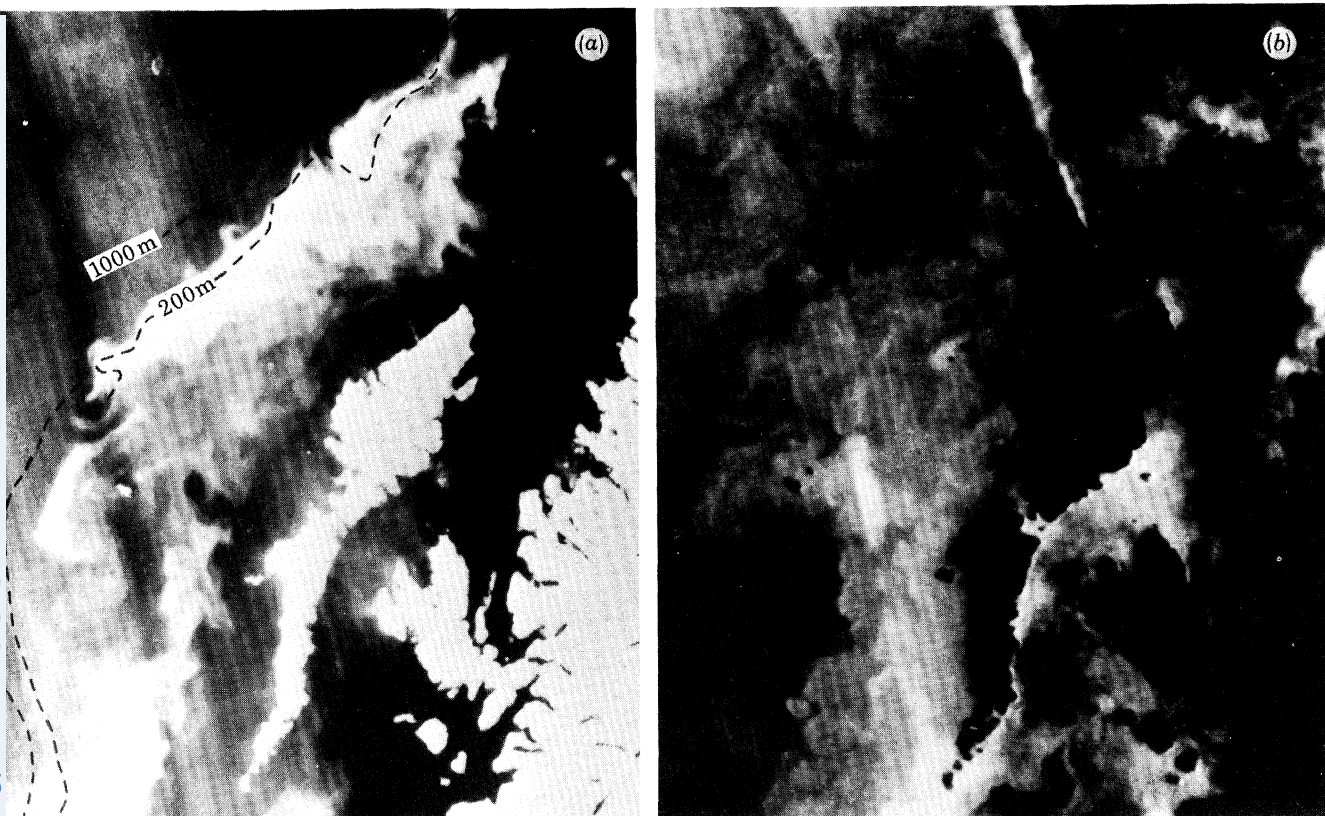


FIGURE 10. (a) Coastal zone colour scanner (c.z.c.s.) image (CH3) of the western (Hebrides) shelf break west of Scotland taken at 11h04 G.M.T. on 17 May 1980 from NIMBUS-7. The scanner is sensitive to chlorophyll or suspended sediments or both. White shading indicates increased chlorophyll in this region. (b) Infrared image of the same region taken from NOAA-6 on 17 May 1980 at 08h49 G.M.T.

The thermocline is also characterized by marked internal wave activity. The broadening of the thermocline over the slopes is thought to indicate more mixing near the shelf break though no bottom-mixed layer has been observed over the slopes.

The surface salinity shows a gradual transition from lower shelf values to higher Atlantic values and is typically 35.5‰ at the shelf break. The salinity minimum at *ca.* 300 m which might reflect an exchange of shelf and slope water results in no density minimum since it occurs

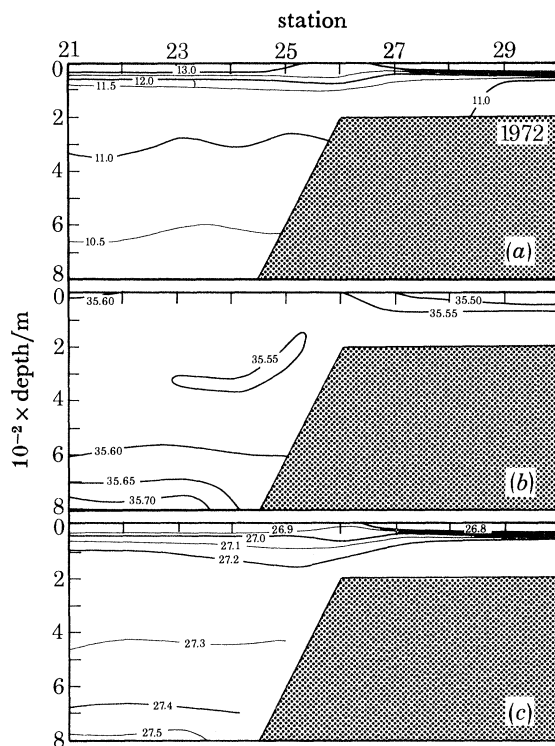


FIGURE 2. STD section completed on 28th June 1972 showing (a) temperature/°C, (b) salinity (‰) and (c) density/ σ_t . Locations of stations 21–30 are shown in figure 1a.

with colder water (not shown in 2a owing to contouring interval). The salinity increases with depth owing to the presence of the core of Mediterranean water centred at a depth of about 900 m.

In September 1973 two further transects were made across the shelf break in the same general area and they showed the same basic features. Two current meter moorings (001, 002) with four current meters on each were deployed near the head of Shamrock canyon to investigate internal waves propagating from the shelf-break region. The results from these, and likely processes leading to nutrient renewal and possible subsequent phytoplankton growth, are discussed later.

During July 1976 a series of surface transects were completed together with a line of stations (1–8) across the shelf break (figure 3). The results show a broad band of cooler water (*ca.* 60 km) centred over the slope region with patches of colder water within this band. The increased fluorescence at the shelf break is partially offset in terms of chlorophyll *a* owing to the high fluorescence–chlorophyll *a* relation for these shelf-break populations (Holligan, this symposium).

The present chlorophyll *a* distributions were derived with local calibrations. Although the chlorophyll *a* and nitrate nitrogen concentrations within this cooler band are low compared with typical surface values found near the neighbouring shelf tidal fronts, they are generally higher than the uniformly low levels commonly observed in the adjacent surface waters of the Celtic Sea and Atlantic Ocean during July. The vertical sections (figure 4) obtained from stations 1–8 show the characteristic chlorophyll *a* maximum associated with the seasonal thermocline. Increased mixing or upwelling in the shelf-slope regions releases nutrients at the surface allowing localized surface phytoplankton blooms to develop under improved light conditions.

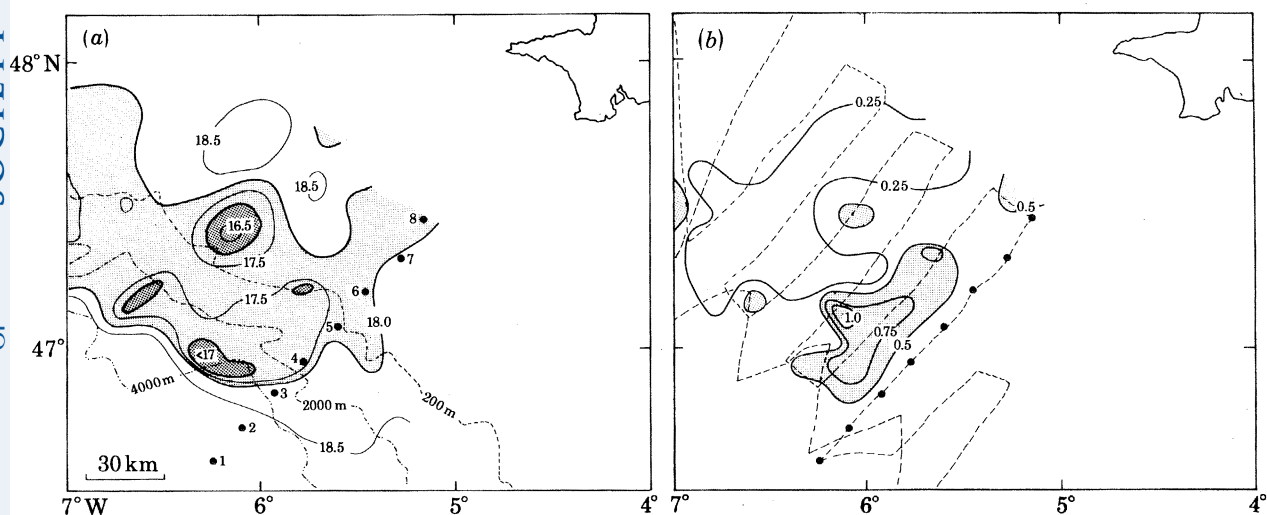


FIGURE 3. (a) Surface (2 m) temperature/ $^{\circ}\text{C}$, (b) surface chlorophyll *a*/ (mg m^{-3}) . Bottom topography in metres is given in (a), and ship's track (July 1976) in (b).

During August 1979 a further interdisciplinary experiment was made to the northwest of the 1976 area (figure 1*a*). The overall surface temperatures were lower than in 1976, although the temperature contrast remained approximately the same (figure 5). The surface salinity ranges from higher oceanic values to lower shelf values with a broader more uniform region (shown shaded in figure 5) over the slope that corresponds to the surface temperature minimum. As in 1976 the surface chlorophyll *a* and nitrate nitrogen concentrations show marginal increases over the slopes and banks. Two current meter moorings (042, 043) were also placed at the shelf break (*ca.* 200 m) (positions $48^{\circ} 41' \text{N}$, $09^{\circ} 36' \text{W}$, $48^{\circ} 51' \text{N}$, $10^{\circ} 02' \text{W}$) and these showed that internal waves were also released in this region.

In August 1980 crossings of the shelf break were completed between the 1976 and 1979 areas (figure 1*a*) together with a line of stations (A–I) along one leg (figure 6). The gross features apparent in previous years can again be recognised. Isolated high nitrate nitrogen patches occur with isolated colder patches, and increased chlorophyll *a* concentrations are associated with the generally cooler water. The vertical cross section stations A–I (figure 7) show the same type of features as observed in previous years, with the chlorophyll *a* concentrated in the thermocline and spreading into the surface layer over the shelf-slope region.

A programme of shelf current meter moorings was made in parallel with the shelf-break studies to investigate the residual currents in the Celtic Sea. The results (figure 8) show that

the residual flows in the Celtic Sea are small (generally less than 5 cm s^{-1}) and that any cross-shelf-break flows associated with these currents will be small and unlikely to affect the dynamics of shelf-break processes, though small subsurface flows may be important in studies concerned with nutrient budgets. In the slope region where the depth is 2000 m the subsurface water (deeper than 250 m) is thought to have a residual flow northwestward of $2\text{--}3 \text{ cm s}^{-1}$ (J. C. Swallow, W. J. Gould & P. M. Saunders 1977, I.C.E.S. CM 1977/C:32, unpublished document).

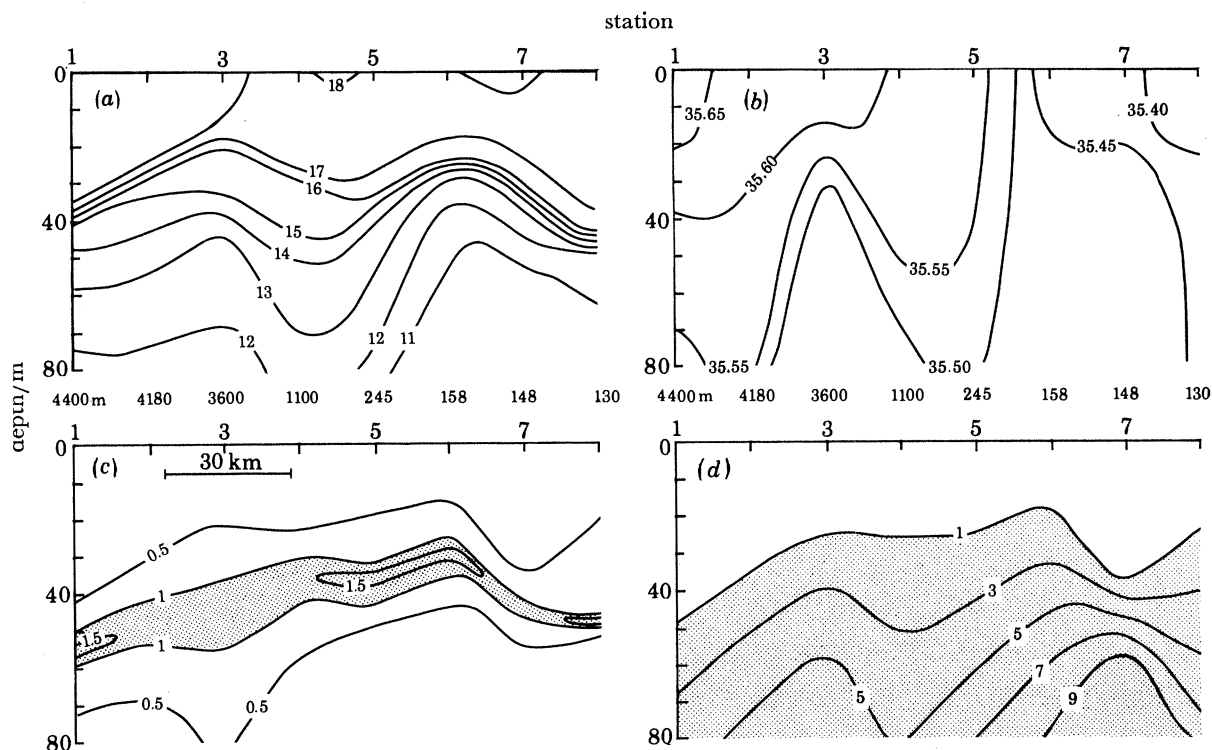


FIGURE 4. Vertical profiles for 1976 drawn from stations 1–8 (figure 3) across the shelf showing (a) temperature/ $^{\circ}\text{C}$, (b) salinity (‰), (c) chlorophyll *a*/ mg m^{-3} and (d) inorganic nitrate/ μM . Numbers between top and bottom parts represent the soundings at each station in metres.

(b) From satellites

The sea programmes were made in conjunction with a study of the available satellite imagery (figure 1*b*). The first satellite images of interest were from the AVHRR sensors aboard NOAA-5, and subsequently from TIROS-N and NOAA-6. They show cooling along the shelf break from May to October (Pingree 1979; Dickson 1980). The band of cooler water is narrow in May when the seasonal thermocline is first established and becomes broader in September reflecting a continuing history of increased mixing in this region. Instabilities at the shelf-break are irregular and rarely show well defined eddies. Like the neighbouring Ushant shelf tidal front the instabilities are more conspicuous in late summer and represent an agency whereby stored potential energy can be released. Instabilities along the Ushant tidal front can take the form of occasional irregular eddies which when apparent are generally cyclonic but sometimes can be anticyclonic or both wound on a common stem. Tidal fronts also show instabilities in the form of intrusive

fingers (up to 30 km long) although these have not been observed at the shelf break. Occasionally there is the suggestion of one or two additional cooler bands of water with a typical spacing of 30 km on the shelf parallel with the shelf break. It is not clear what relation these features have with the shelf break.

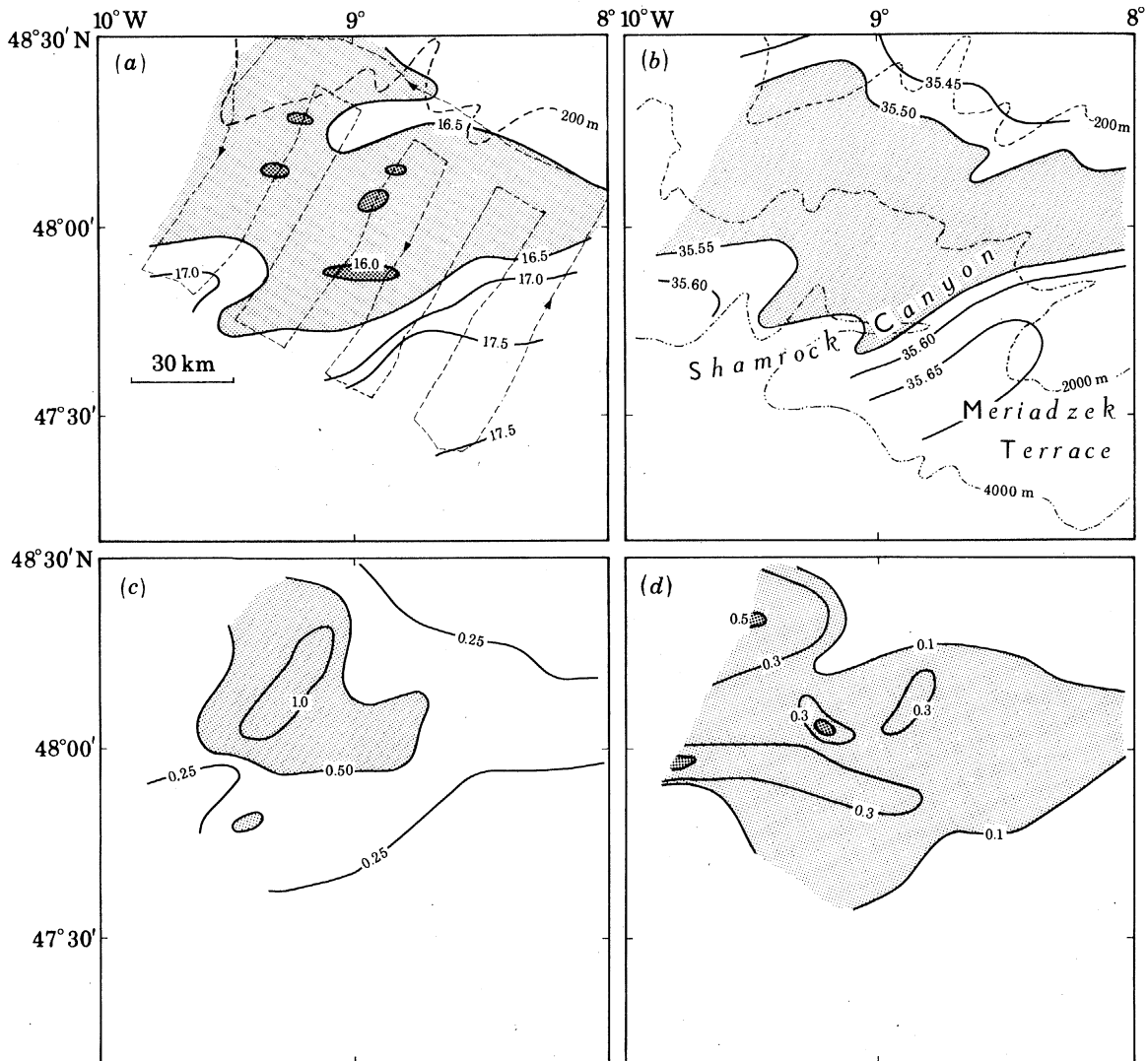


FIGURE 5. (a) Surface temperature/ $^{\circ}\text{C}$, ship's track; (b) salinity (‰); (c) chlorophyll *a*/ mg m^{-3} ; and (d) inorganic nitrate/ μM (August 1979). Bottom topography is given in metres.

In addition to infrared imagery, use was made of the synthetic aperture radar (s.a.r.) on board SEASAT. Although this satellite only operated for a short time it provided a very good pass across the Bay of Biscay from Brest to Corunna, part of which is illustrated in figure 9*a*. Variations in sea surface roughness allow the radar to show surface swell (*ca.* 200 m wavelengths) and internal waves (longest wavelengths *ca.* 2 km). The swell at the shelf break is propagating along the slope direction in the general wind direction which was northwesterly (*ca.* 5 m s^{-1}) at the shelf break owing to a high pressure ridge to the west at that time.

It is not thought that the surface swell is significant in the generation of the internal waves seen in the s.a.r. image near the shelf-break and in the adjacent region of the North Atlantic. The internal waves appear as sets of intersecting arcs which seem to be propagating from topographic features in the general vicinity of the shelf break. These arcs may intersect and give an impression of a more general internal wave front propagating out into the Atlantic near the 700 fathom (1281 m) contour. A further more general disturbance occurs near the 100 fathom

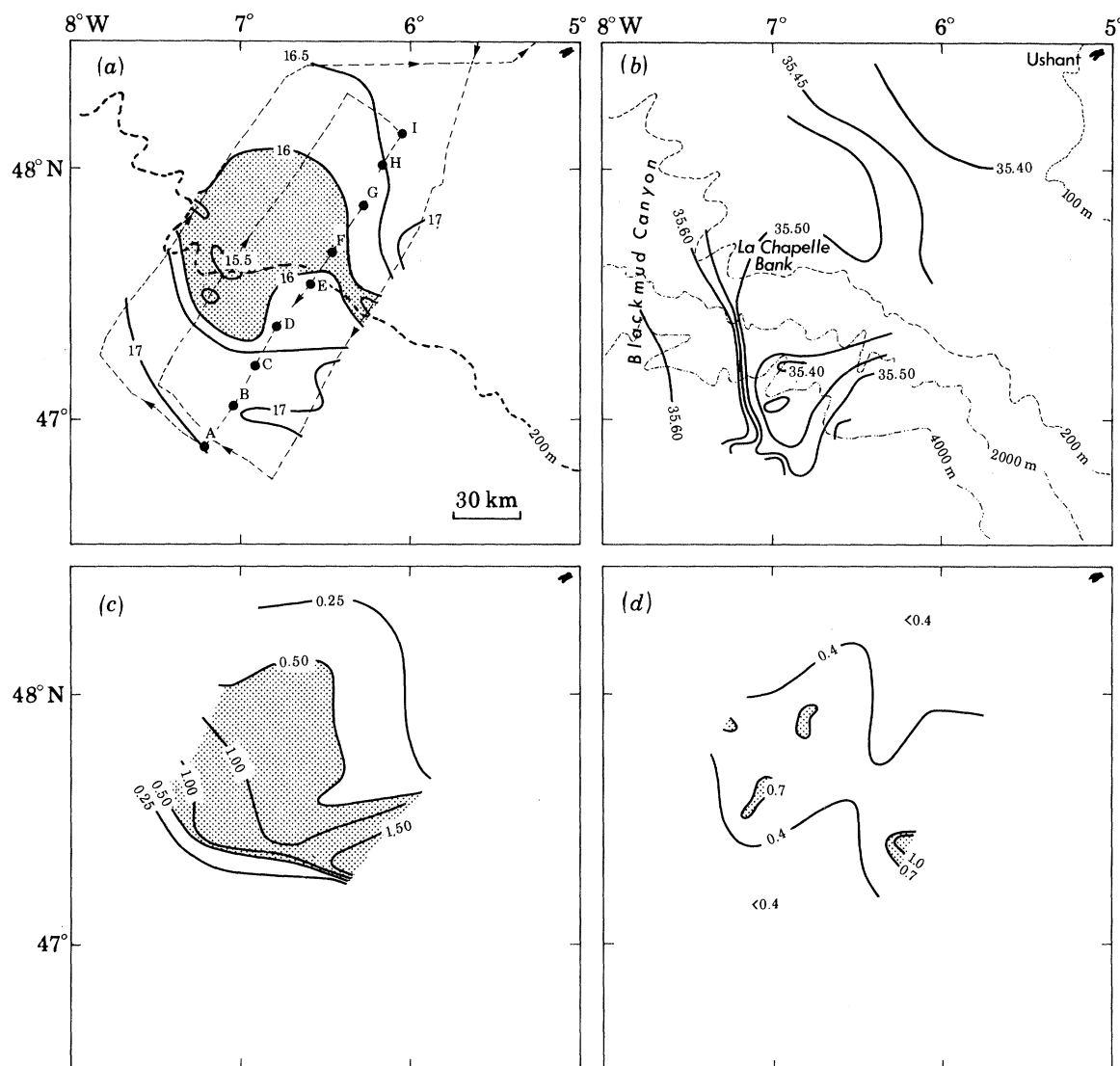


Figure 6. (a) Surface temperature/ $^{\circ}\text{C}$, ship's track, (b) salinity (‰), (c) chlorophyll a / (mg m^{-3}) and (d) inorganic nitrate/ μM (August 1980). Bottom topography is given in metres.

(183 m) contour. In this region of the Armorican shelf internal waves appear to propagate out into the Atlantic more readily than on to the shelf though some internal waves can clearly be seen propagating on-shelf (figure 9*b*). The region of shelf-break cooling corresponds approximately to the region of marked internal wave activity and suggests that the disturbances that cause the internal waves or the shear associated with internal waves may play a key role in slope

mixing processes. The density structure of shelf-break frontal zones may in turn affect the propagation of internal waves out from the shelf-break slope region.

It is interesting to note that no marked internal waves were observed at the southern end of the s.a.r. pass near the Spanish coast though some isolated weak disturbances could be observed. The s.a.r. image coincided with spring tides, and if these features are of tidal origin it seems unlikely that internal waves propagating out into the Atlantic from the shelf break will be significant in the southern Biscay. Although the southern end of this pass is close to a region of marked upwelling off Cape Finisterre no shelf-break cooling has yet been observed here.

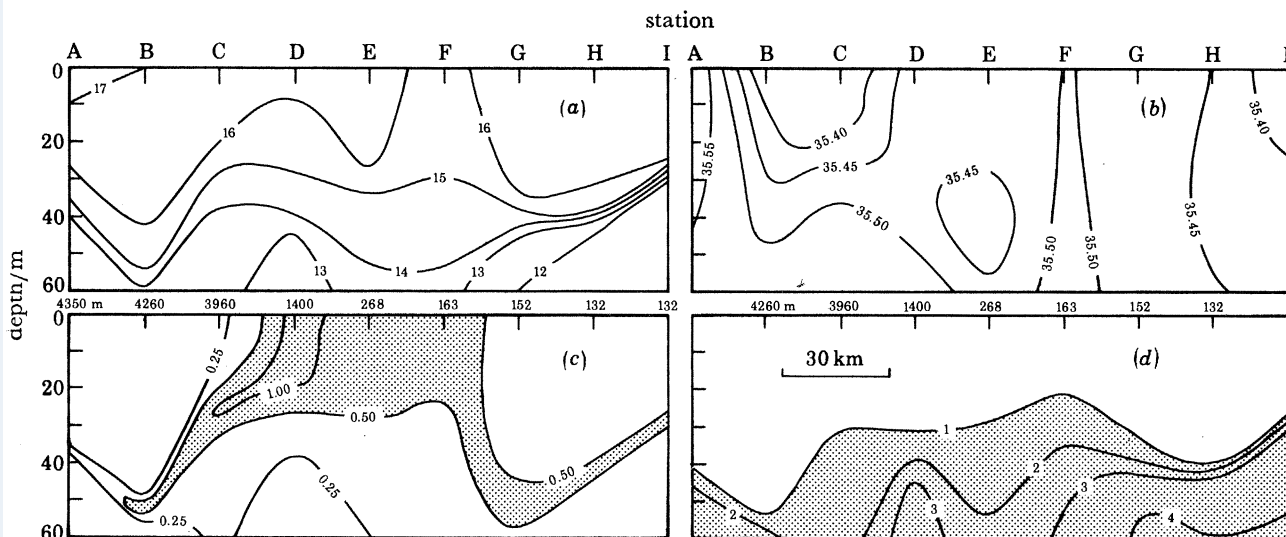


FIGURE 7. Vertical sections drawn from stations A–I (figure 6) of (a) temperature/ $^{\circ}\text{C}$, (b) salinity (‰), (c) chlorophyll *a*/ mg m^{-3} , and (d) inorganic nitrate/ μM . Depths are in metres. Numbers between top and bottom parts represent the soundings at each station in metres.

Other types of remote sensors can also be useful in these studies, one of which is the recently available coastal zone colour scanner (c.z.c.s.) on NIMBUS-7. This can highlight areas of interest that are not apparent in infrared imagery. An example is given in figure 10 (plate 2) which shows the shelf break off northwest Scotland sensed by NIMBUS-7 only 2.25 h after NOAA-6. The normal infrared images from NOAA-6 reveal a temperature gradient from cold shelf waters to warmer oceanic waters at the shelf break, with no obvious temperature minimum suggesting enhanced mixing or upwelling at the slope. However the c.z.c.s. image from NIMBUS-7 reveals a definite white band along the edge of the shelf. This region of increased chlorophyll suggests that some upwelling or increased mixing leading to nutrient renewal had previously taken place at the shelf break in this region.

DISCUSSION

The cooler band of surface water at the shelf break may be attributed to a number of different mechanisms owing to the complex motions that can occur in a stratified fluid along a steeply sloping shelf (J. M. Huthnance 1980 I.O.S. Rep. no. 97 (unpublished)). These motions which may be initiated by weather or tides or a combination of both are discussed in further

detail in the following paragraphs, as they provide the physical framework in which to view shelf-break production.

Internal waves

Internal waves are a universal feature of the oceans, but their occurrence on the continental shelves will depend on the stratification there, and on any transmission or generation near the shelf edge (Apel 1975). It can be seen clearly in the s.a.r. image that some of these internal waves

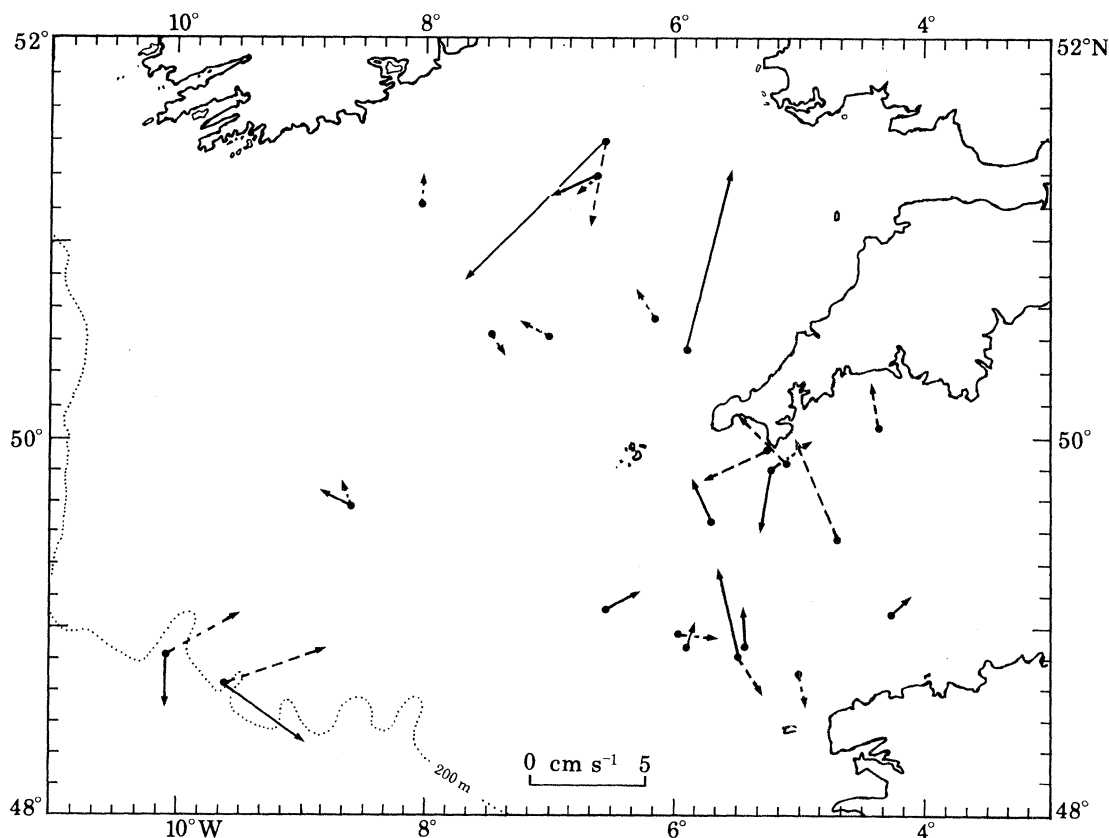


FIGURE 8. Residual flows from moored current meter stations measured over periods between 1 and 4 months. The length and orientation of the arrows represent the average distance and direction of water movements over a period of about 15 days. Solid arrows represent surface flow and dotted arrows represent bottom mixed layer flows.

are generated near the 100 fathom (183 m) contour (Mazé 1980). The phase velocity c for linear internal waves in a two-layered system is obtained from the following formula where rotational effects are neglected and the fluid is assumed confined between rigid horizontal planes at the surface and the bottom:

$$c^2 = g\Delta\rho/k (\rho_0 \coth kh_0 + \rho_1 \coth kh_1)^{-1} \quad (1)$$

where $\Delta\rho = \rho_1 - \rho_0$, $k = 2\pi/\lambda$, c is the phase velocity of the internal wave, λ is the wavelength of the internal wave, h_0 is the depth of the layer above the thermocline, h_1 is the depth of the layer below the thermocline, ρ_0 is the density of the layer above the thermocline, ρ_1 is the density of the layer below the thermocline, g is the acceleration due to gravity.

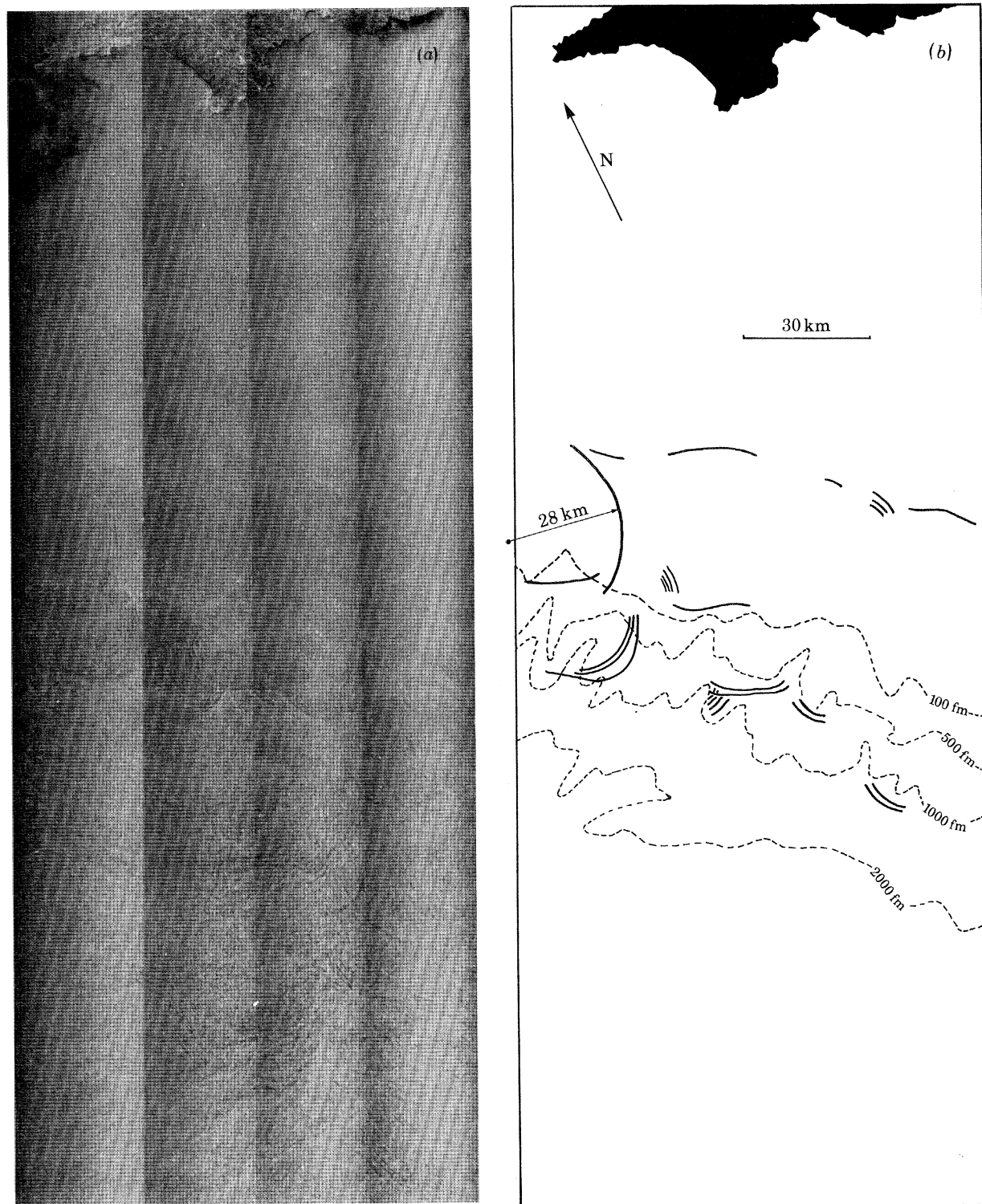


FIGURE 9. (a) Part of a synthetic aperture radar (s.a.r.) pass from SEASAT on 20 August 1978. For location see figure 1a. (b) Stylized pictures of the main features of interest in figure 9a. Depths are in fathoms (fm) owing to the use of chart C6568 (1 fm = 1.83 m).

The internal waves are long (*ca.* 1 km) compared with the shallow seasonal thermocline at a depth of 30–50 m and so the internal waves on the seasonal thermocline tend to be non-dispersive, though the longest wave tends to lead. Characteristic phase velocities are of order 40–60 cm s⁻¹ with typical shelf summer temperature differences of 3–6 °C (salinity effects on the shelf are generally negligible). At the shelf break it will be more appropriate to adopt a formulation for the phase speed that takes account of the vertical density structure.

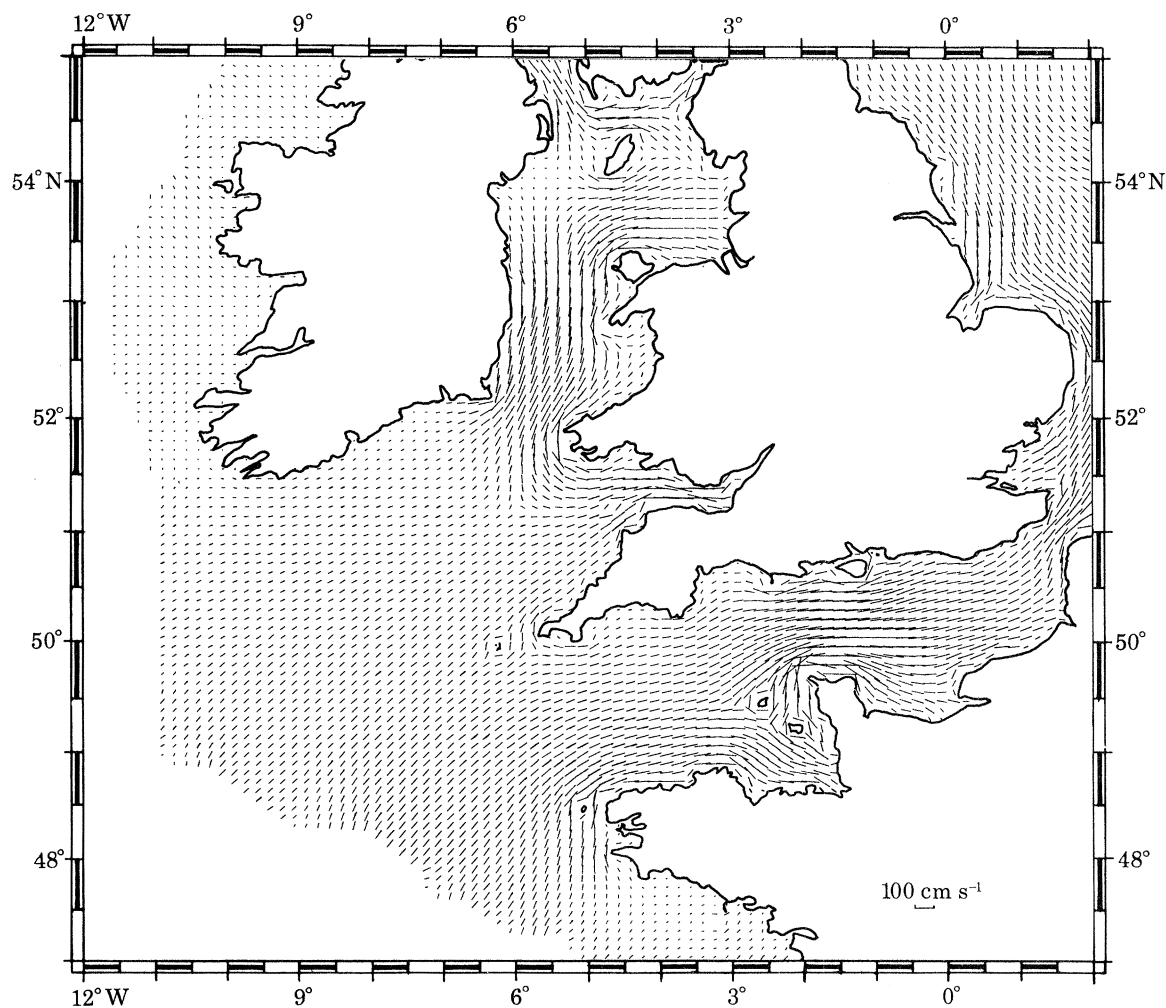


FIGURE 11. M_2 tidal currents, semi-major axis (numerical model (Pingree & Griffiths 1978)).

It is thought that the internal waves generated near the shelf-break (as observed in the s.a.r. image) are of tidal origin. The M_2 tidal currents on the shelf near the Celtic Sea shelf-break are generally rotatory (clockwise) with a ratio of minor to major axis of about 60–70%. The tidal wave is partially progressive to supply an energy flux to balance the marked tidal dissipation that occurs in the English Channel and Irish Sea. The maximum streams are aligned approximately perpendicular to the shelf break, with typical vertically integrated M_2 currents of 20–55 cm s⁻¹ (figure 11). Maximum semidiurnal currents will occur when M_2 , S_2 , N_2 and K_2 constituents are in phase with $33\% \lesssim S_2/M_2 \lesssim 38\%$, $N_2/M_2 \approx 20\%$ and $28\% \leq K_2/S_2 \lesssim 29\%$ so the maximum permissible semidiurnal currents will be about $\frac{5}{3}$ the values derived from

figure 11, and will tend to occur either before the thermocline is established or near the final stages of erosion when the K_2 can be in phase. In the deeper water over the slopes the tidal currents diminish rapidly owing to continuity effects with M_2 currents typically about 5 cm s^{-1} in water depths of *ca.* 2000 m (Gould & McKee 1973).

The semidiurnal tides might create standing internal lee waves when flowing west over the shelf edge, and these could travel across the shelf first after maximum streaming and then assisted by the on-shelf tide. Internal waves propagating from the shelf break into the deeper Atlantic may be due to general slope disturbances, perhaps associated with trapped waves, or

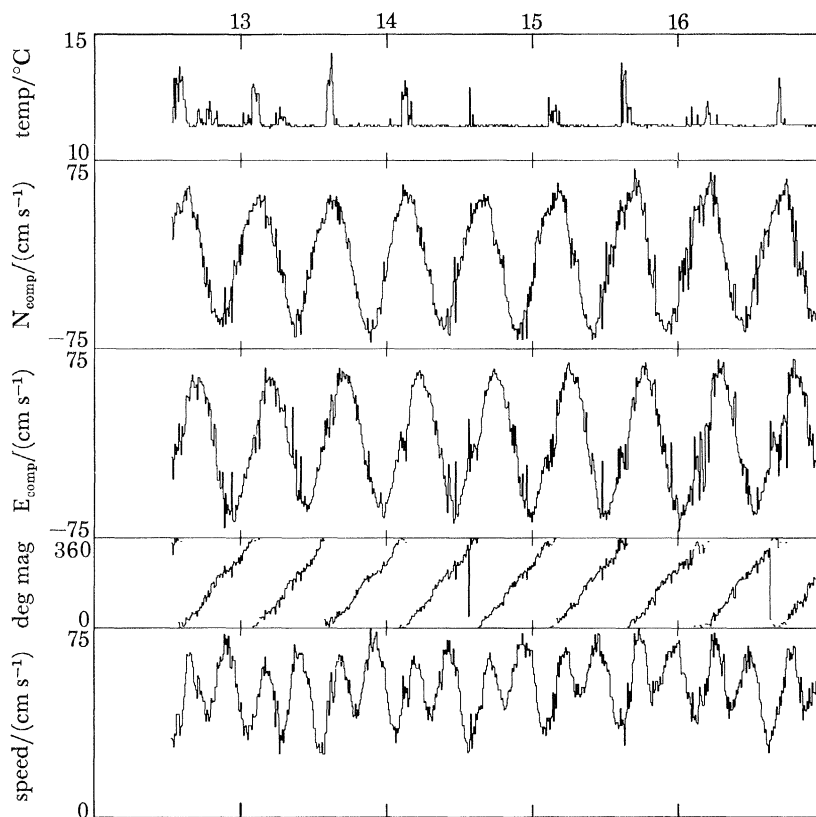


FIGURE 12. Current meter record from current meter 98 m off bottom on mooring 001 ($48^\circ 10.5' \text{ N}$, $7^\circ 53.5' \text{ W}$).

may occur as on-shelf tidal streaming slackens. The s.a.r. image suggests predominantly off-shelf propagation though it is clear from the current meter moorings that marked on-shelf propagation can also occur.

In September 1973 two current meter moorings (001, 002) were deployed normal to the shelf break and separated by 13.5 km near Shamrock Canyon (figure 1*a*) where the M_2 tidal currents reach their maximum (figure 11). Mooring 001 laid near by in a depth of 188 m showed that internal waves passed this mooring about 1–2 h after the tide started streaming on-shelf (figures 12, 13). At the second mooring 002 in a water depth of 184 m internal waves were first observed about 3.2 h later (figure 13), which is consistent with the view that internal waves propagate on-shelf with on-shelf tidal streaming. The water particle velocities of the internal waves estimated from the current meter records in the bottom-mixed layer at mooring 001 (see figure 14) gave speeds of $10\text{--}30 \text{ cm s}^{-1}$, and their directions suggested that at the time these waves passed

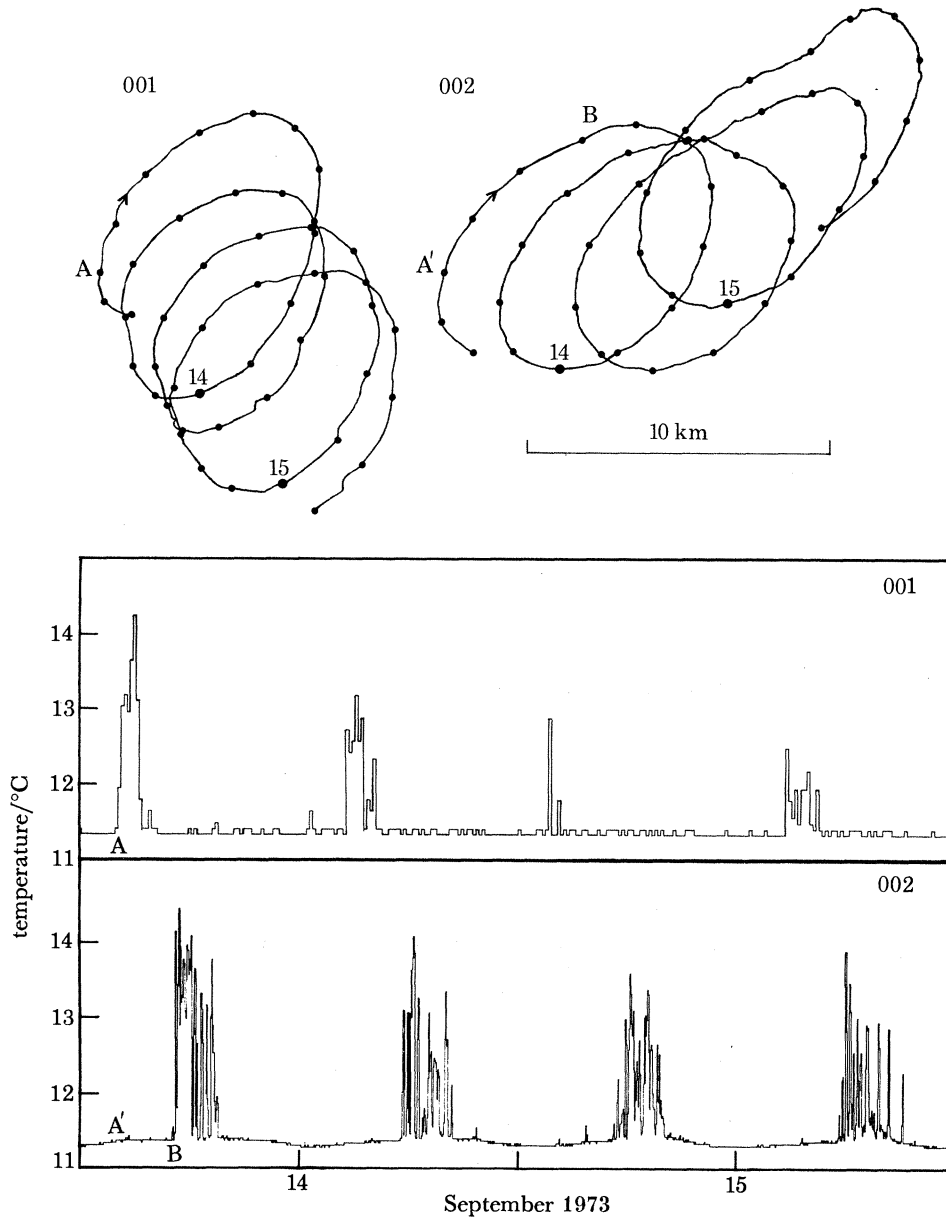


FIGURE 13. Temperature traces and progressive vector diagrams for current meters 98 m off the bottom on mooring 001 ($48^{\circ} 10.5' N$, $7^{\circ} 53.5' W$, water depth 188 m) and 002 ($48^{\circ} 16.5' N$, $7^{\circ} 47' W$, water depth 184 m). Internal waves first recorded at 001 at time A were first observed at time B at 002 about 3.2 h later. The current meter records were 7 days long and the spring tide period is illustrated.

mooring 001 they were propagating at an angle of $20\text{--}40^{\circ}$ to the line joining the two mooring positions. If it is assumed that the internal waves passing 001 and 002 have a common source, and allowance is made for the fact that in 3.2 h the tide moves about 6.5 km on-shelf, then an estimate for the phase speed becomes 60 cm s^{-1} , which is in approximate agreement with a value of *ca.* 55 cm s^{-1} determined from the density structure at the time of the observations (see equation (1)). At mooring 001 the internal wave is a large depression of the seasonal thermocline whereas at 002 the major disturbance is smaller and tends to be followed by a train of shorter waves (Djordjevic 1978) (figure 13, for example, on the morning of 15 September

1973). Allowing for the tide gives a period of *ca.* 30–40 min for these shorter waves, and using a phase velocity of *ca.* 60 cm s⁻¹ makes the wavelength about 1–1.5 km, which is in broad agreement with the features seen in the s.a.r. image.

Internal waves are likely to cause increased mixing in the thermocline if the local Richardson number becomes small and perhaps at the shelf tidal fronts exposed to internal wave attack, and may be important in maintaining a nutrient supply for phytoplankton. In addition, variations

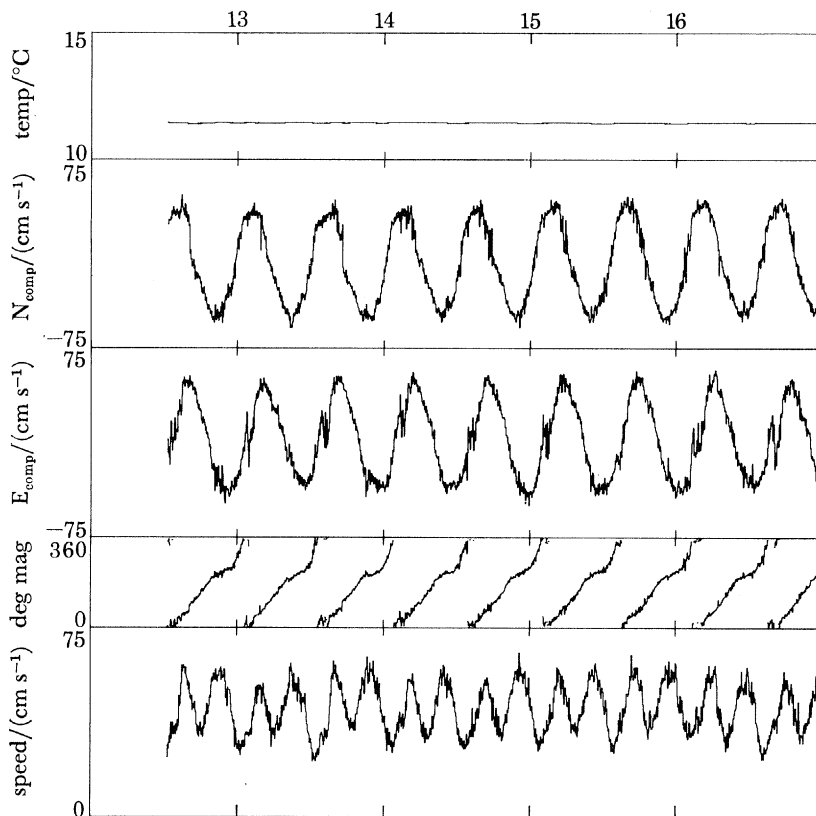


FIGURE 14. Current meter record from current meter 33.5 m off bottom in the bottom-mixed layer on mooring 001 (48° 10.5' N, 7° 53.5' W).

in light intensity due to variation in the depth of the thermocline may be important in determining the availability of light energy for thermocline phytoplankton populations. The peak-to-trough amplitude of the shelf-break internal waves near moorings 001, 002 can be *ca.* 50 m though the major on-shelf internal wave generated near the 100 fathom (183 m) contour is one of depression rather than elevation in this region.

The water particle velocities in the shallow upper layer ($h_0 \approx 40$ m) can be expected to be larger than those in the deep bottom-mixed layer. An estimate for a minimum Richardson Number, Ri , with maximum shear Δu (*ca.* 50 cm s⁻¹) across the thermocline Δz (*ca.* 20–40 m) gives

$$Ri = \frac{g}{\rho} \frac{\Delta \rho}{\Delta z} / \left(\frac{\Delta u}{\Delta z} \right)^2 \approx \left(\frac{c}{\Delta u} \right)^2 \frac{\Delta z}{h_0} \approx 1.$$

Although this value is low it is larger than typical values suggested for instability. Mixing might occur in the processes leading to the formation of these internal waves at the shelf break or where different large-amplitude internal wavetrains interfere.

The decay time-scale for internal waves propagating on the shelf will depend on divergence, dispersion, internal friction and bottom friction. The latter will depend on the tidal currents (u_T , figure 11) and is of order $h_1/C_D u_T \approx 1$ day (with drag coefficient $C_D \approx 0.0025$, $u_T \approx 40 \text{ cm s}^{-1}$).

Trapped waves

The steep slopes near the shelf-edge imply a large potential vorticity gradient. A fluid column displaced up or down the slope, and conserving potential vorticity, acquires relative vorticity. Horizontal shear at the shelf break, perhaps due to wind stress, can result in a long-shelf propagation of the disturbance in a cyclonic sense about the deeper water. Thus these waves in the Northern Hemisphere must travel with the shallow water to the right and hence propagate northwest along the Celtic Sea shelf break. Such wave motions are known as continental shelf waves (Robinson 1964). In stratified conditions the shorter wavelengths may take the form of bottom-trapped waves.

Slope roughness is likely to interact with diurnal and shelf waves to promote mixing. It is thought that locally enhanced upwelling can occur when these waves encounter ridges and canyons (Kilworth 1978). In addition internal waves may be generated and propagate away from the mixing sites.

Upwelling

Heaps (1980) has proposed that the sea-surface cooling along the slopes is due to upwelling rather than enhanced mixing or wave activity in the slope region. Instead of the more usual mechanisms of wind-induced upwelling he argues that the marked thermocline on the shelf allows more shear in the shelf surface waters than in the more diffusive thermocline over the slopes under on-shelf wind conditions. This is thought to result in upwelling at the shelf break. Although this seems likely it is noticeable that the shelf-break cooling, as identified in infrared imagery, is particularly conspicuous during high pressure, low wind conditions. It might be argued that downwelling should also occur where the oceanic seasonal thermocline borders the more diffuse slope thermocline.

Geostrophic flow

The surface cooling due to increased mixing at the shelf-break indicates a region below the surface where there is a wider separation of the isopycnals than in the oceanic or shelf seasonal thermocline. If this more mixed zone is assumed to be in geostrophic balance then it will be moving northwestward on the oceanic side and southeastward on the shelf side relative to the oceanic and shelf water respectively. A batfish run giving the density structure across the shelf break in the 1980 survey (figure 6) was used to calculate the geostrophic shear. It gave typical values of $1\text{--}3 \text{ cm s}^{-1}$ for the northwesterly flow and similar values for the southeasterly flow. The zone of increased fluorescence at the shelf break might therefore be subjected to a general weak anticyclonic shear.

CONCLUSION AND SUMMARY

Measurements at sea, over the period 1972–80, and observations from space have concentrated on those shelf-break and slope processes thought to be important in determining the increased fluorescence commonly observed along the Celtic Sea shelf break during the summer. In June 1972 a vertical section of the shelf-slope region revealed a general sea-surface cooling over the slope region with marked internal wave activity on the thermocline at the shelf break and a well defined bottom-mixed layer (*ca.* 100 m) on the shelf caused by tidal stirring. In

September 1973 further sections showed the same general surface cooling (*ca.* 1 °C) over the slopes, and two current meter moorings were deployed to study the propagation of internal waves on to the shelf from the shelf break near Shamrock Canyon. In summer, in this region, the on-shelf internal waves can have a maximum trough amplitude of *ca.* 40 m. They are released from the shelf break with semidiurnal tidal period and propagate on-shelf with typical phase velocities of 20–30 km per semidiurnal tidal period.

The results were subsequently highlighted and given increased significance when in 1976 infrared satellite images showed that summer cooling could on occasions extend for 800 km along the Armorican and Celtic Sea slopes. The band of cooler water tends to be narrow in May and broader in September. The increased mixing at the shelf break is partially stored as potential energy which may be released in the form of irregular baroclinic eddies along the slope region in late summer. In addition to infrared imagery, SEASAT s.a.r. images (1978) revealed marked internal wave activity in this region. Internal waves could be seen propagating out into the Atlantic mainly from the shelf-slope region with some on-shelf propagation. The increased internal wave activity at the shelf break could be continuous for distances of up to 100 km, and the results from moorings 001, 002, 042, and 043 suggest these effects may stretch for 400 km or more along the shelf-break region.

Interdisciplinary studies of the shelf-break region were started in 1976 with further studies in 1979 and 1980. They showed the slopes to be characterized by increased levels of surface fluorescence and traces of inorganic nutrients detectable in the surface waters over the shelf-slope region. The increases in fluorescence and nutrients are attributed to the mixing processes operating at the shelf break which mix up phytoplankton and nutrients, from the thermocline and below, into the surface waters.

Mixing caused by the barotropic tide in generating internal waves at the shelf-break (Zeilon 1912) appears to play a role in shelf-break cooling and nutrient release. In addition to wind-induced upwelling, enhanced mixing and upwelling is also likely to occur along the slopes where slope roughness (canyons and ridges) interacts with trapped waves propagating along the slope. Increased phytoplankton growth may then take place under improved light conditions where nutrients and phytoplankton are released into the surface waters along the shelf-break region of the Celtic Sea.

REFERENCES (Pingree & Mardell)

- Apel, J. R., Burne, H. M., Prioni, J. R. & Charnell, R. L. 1975 *J. geophys. Res.* **80**, 865–881.
 Dickson, R. R., Gurbutt, P. & Pillai, V. 1980 *J. phys. Oceanogr.* **10**, 813–819.
 Djordjevic, V. C. & Redekopp, L. G. 1978 *J. phys. Oceanogr.* **8**, 1016–1024.
 Gould, W. J. & McKee, W. D. 1973 *Nature, Lond.* **244**, 88–91.
 Heaps, N. S. 1980 *Oceanologica Acta* **3**, 449–454.
 Killworth, P. D. 1978 *J. phys. Oceanogr.* **8**, 188–205.
 Laughton, A. S., Roberts, D. G. & Graves, R. 1975 *Deep Sea Res.* **22**, 791–810.
 Mazé, M. R. 1980 *Annls hydrogr.* **754**, 45–58.
 Pingree, R. D. & Griffiths, D. K. 1974 *Nature, Lond.* **250**, 720–722.
 Pingree, R. D. & Griffiths, D. K. 1978 *J. geophys. Res.* (Chapman Conference Issue) **83**, 4615–4622.
 Pingree, R. D. 1979 *J. mar. biol. Ass. U.K.* **59**, 689–698.
 Robinson, A. R. 1964 *J. geophys. Res.* **69**, 367–368.
 Zeilon, N. 1912 *K. svenska. VetenskAkad. Handl.*

Discussion

D. E. CARTWRIGHT (*Institute of Oceanographic Sciences, Bidston Observatory Birkenhead, Merseyside L43 7RA, U.K.*). Tidally generated internal waves at or near La Chapelle Bank were first

measured by sonic sounding of the scattering layer by Stride & Tucker (1960), and I was present on the last cruise of R.R.S. *Discovery II* in 1962 when large internal temperature fluctuations were recorded in the same area from a towed thermistor chain (Bowers & Bishop 1966). In both cases the internal waves were clearly of the same length as the giant sand-waves which are now well known along that shelf edge, so one wonders if the sand waves play some part in triggering off the internal wave motion and consequent mixing at critical states of the tidal stream. I have analysed a mechanism for how such sand-waves may be formed (Cartwright 1959) but my question is this: Given the sand waves, is there any evidence that they provoke the observed turbulence in the tidal streams, or does the turbulence occur equally at parts of the shelf edge where there are no sand waves?

References

- Bowers, R. & Bishop, D. G. 1966 In *Proc. I.E.R.E. Conf. Electronic Engineering in Oceanography*, Southampton, 1966, pp. 711–714.
 Cartwright, D. E. 1959 *Proc. R. Soc. Lond.* **A253**, 218–241.
 Stride, A. H. & Tucker, M. J. 1960 *Nature, Lond.* **188**, 933.

R. D. PINGREE. Internal waves associated with the shelf break have been well known since the studies of Zeilon (1912). Significant contributions to the on-shelf propagation of internal waves from space were made by Apel *et al.* (1975). Our experiments were made in 1973 after a suggestion of Dr L. H. N. Cooper, F.R.S., who wrote several stimulating papers (Cooper 1947, 1952*a*) on the importance of internal waves in this area. Our studies showed on-shelf propagation of wave packets with on-shelf tidal streaming, but no submarine eages propagating from submarine canyons (Cooper 1952*b*) have yet been found. It is not clear from our results that the internal waves are generated by sand waves and that the sand waves in this area are in turn generated by internal waves as proposed by Dr Cartwright. The internal waves measured by sonic sounding in the paper to which Dr Cartwright refers appear to be of smaller amplitude and wavelength than the features described in the text. How sure are you that the internal waves at or near Chappelle Bank have the same wavelength as the sand waves? To what accuracy can you estimate the wave number and direction (i.e. directional wave number spectrum) of the internal waves and the sand waves? The mixing efficiency of internal waves in this region is unknown though an energy budget relating the internal wave energy flux to the change of potential energy of the water column is outlined in the reply to Dr Peregrine's comment below.

In the intervening years since Zeilon's pioneering studies many important questions concerning shelf-break internal waves have naturally been raised. We now have the opportunity to examine these processes in more detail in the recently proposed northwest European slope-shelf-break experiment in which I.O.S. Bidston is playing a leading role.

References

- Cooper, L. H. N. 1947 *Nature, Lond.* **159**, 579.
 Cooper, L. H. N. 1952*a* Processes of Enrichment of water with nutrients due to strong winds blowing on to a continental slope. *J. mar. biol. Ass. U.K.* **30**, 453–464.
 Cooper, L. H. N. 1952*b* *J. mar. biol. Ass. U.K.* **31**, 351–362.
 Zeilon, N. 1912 *K. svenska. Vetenskakad. Handl.*

D. H. PEREGRINE (*School of Mathematics, University of Bristol, Bristol BS8 1TW, U.K.*). A distinctive feature of the measurements presented is that the thermocline over the continental shelf

slope is very much thicker than it is either over the oceanic deeps or the continental shelf. An explanation of this feature might be found by investigating the propagation of internal waves on the thermocline. Internal waves over the continental shelf are propagating on tidal currents which have velocities of the same order of magnitude as the phase velocities of the internal waves. When these currents are taken into account I expect that the internal wave field would have many features in common with surface waves on currents.

The most relevant property for this case is the short wave singularity that occurs when waves are being swept downstream by a current to a region where that current drops to near near-zero speed. This is illustrated, without comment, in figures 4 and 11 of Peregrine (1976), and figure 6 of the same paper is a sketch of a more complicated, but more general example, of wave refraction by a non-uniform current which leads to a considerable reduction in wavelength. More details of the case of a directly adverse current are given in Peregrine & Thomas (1979). Some aspects of the general problem are discussed in Peregrine & Smith (1979).

On the continental slope there is a relatively high gradient of tidal current, and it is likely that a high proportion of the internal waves swept into that region off the shelf suffer a substantial reduction of wavelength. This leads to the waves' kinetic energy being concentrated nearer to the thermocline and probably to a substantial loss of energy by breaking. Breaking occurs at the thermocline and much of the energy is directly available for mixing: this broadens the thermocline.

Even without currents the thicker thermocline could cause incident internal waves to break. The waves propagate slower on the broader thermocline and become shorter and steeper, to maintain the same wave action flux.

Observations clearly show that some strong internal wave activity is generated by the tidal currents. Any non-uniformity in the bed leads to generation of stationary waves on a uniform current of Froude number near unity. If the current varies in time, as in this case, the waves so generated become freely propagating waves. Since such waves originate with their group velocity less than the current velocity, they have a very good chance of being swept to the shelf edge and hence contributing to mixing in the thermocline.

Observations at a single station are unlikely to provide much information on the internal wave properties, even if the current is measured and the thermocline tracked in time. More extensive observations are needed to assess the orientation of the internal waves. Satellite and aerial photographs are likely to show only the largest waves but could be very helpful in indicating the scatter of wave directions.

References

- Peregrine, D. H. 1976 *Adv. appl. Mech.* **16**, 9–117.
 Peregrine, D. H. & Smith, R. 1979 *Phil. Trans. R. Soc. Lond. A* **292**, 341–370.
 Peregrine, D. H. & Thomas, G. P. 1979 *Phil. Trans. R. Soc. Lond. A* **292**, 371–390.

R. D. PINGREE. Much of Dr Peregrine's comment is concerned with internal waves propagating towards the slopes where increased mixing may take place on account of adverse currents (considered by Phillips *et al.* 1968) or a broadening of the thermocline. The broadening of the thermocline will enhance the amplitude of the internal wave, thereby increasing the likelihood of wavebreaking. Thus an interesting feedback mechanism may operate once conditions are suitable for the wave-breaking process to begin. Undoubtedly these effects will be important in

some regions though other considerations seem more relevant at the Celtic Sea shelf break. While it is true that current meter moorings may not provide much information on the internal wave properties they are currently the only direct measurements we have. In the region near Shamrock canyon they have provided the amplitude, phase speed, wave number and direction of the internal waves. Perhaps most important of all is that the measurements have shown that the large amplitude internal waves in this region are phase-locked with the tide. That is, they appear to be generated during maximum off-shelf tidal streaming from localized sources (though not necessarily sand waves) and propagate on-shelf with on-shelf tidal streaming. Although the s.a.r. image shows general internal wave activity in the oceanic waters, near the slopes the internal waves appear to propagate out into the deep ocean. It is therefore our opinion that the shelf-slope region is a source of internal waves rather than a sink region as implied by Dr Peregrine. The question naturally arises as to whether the internal waves generated near the shelf break are capable of providing sufficient mixing to broaden the thermocline or whether the broadening is simply a by-product of some other more efficient mixing or upwelling process that may also cause internal waves. To examine the effectiveness of internal waves in mixing water near the shelf break it is instructive to consider an energy balance between the observed change in potential energy of the water column and the proportion of the internal wave energy flux that is available for mixing. This was suggested to us by Dr Thorpe and essentially reproduced in the following section.

The energy flux is Ec_g per unit length normal to the group velocity, c_g , where E is the energy of the waves per unit surface area. If a fraction α is transferred into potential energy when the waves break and dissipate all their energy over a region of scale l then the rate of change of potential energy per unit area is $\alpha Ec_g/l$. To see whether this is significant calculate how long it would take to cause the potential energy difference observed in the relatively mixed zone with respect to the surrounding regions. This change (per unit surface area) is about $g\Delta\rho d^2/24$, where $\Delta\rho$ is the density difference between top and bottom and d is the thickness of the thermocline in the slope region. The time, T , needed for the internal waves to cause such mixing over the region of scale l , if they are present for a fraction f of each tidal cycle, is

$$T \approx \Delta\rho g d^2 l / 24 \alpha E c_g f.$$

If $E \approx \frac{1}{2} g \Delta\rho a^2$ and $c_g \approx \lambda/n\tau$ ($1 < n < 2$), where a is the internal wave amplitude, λ , τ the wavelength and period respectively, then the time needed is

$$T \approx \frac{nd^2l\tau}{12\alpha a^2\lambda f}.$$

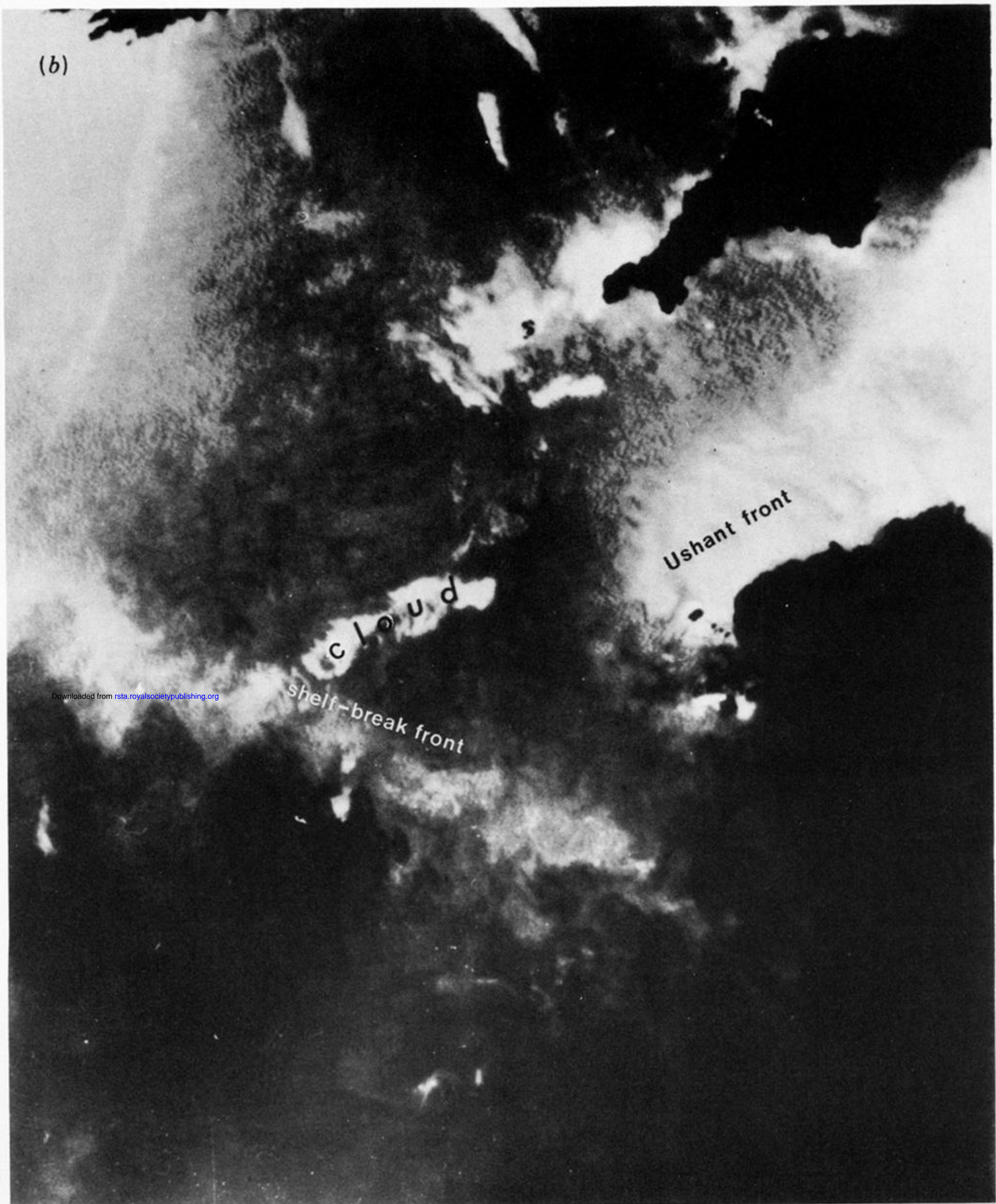
Assume that the internal waves propagate alternately on-shelf and off-shelf from the shelf break after maximum tidal streaming, then l might be taken as half the scale of shelf-break cooling. Suitable values are $l \approx 25$ km, $n \approx 1$, $d \approx 80$ m, $\tau \approx 30$ min, $\alpha \approx 0.1$, $a \approx 20$ m, $\lambda \approx 1$ km and $f \approx 0.1$ so that $T \approx 70$ days.

While such an estimate indicates that internal waves must be considered as a serious candidate for shelf-break cooling, the derived result can be modified and improved on several accounts. The most important aspect is perhaps that in addition to a time factor f (which may vary during a springs-neaps cycle) a further spatial factor is required. The real situation is indeed further complicated by the fact that the internal waves appear to originate from localized sources and that the disturbances can interfere in some regions and are absent in others. Moreover there is

no evidence that the internal waves propagating off-shelf are tidally generated. Nevertheless the above energy argument is presented as the major contribution to this discussion since it clearly identifies areas where further research is necessary.

Reference

Phillips, O. M., George, W. K. & Meid, R. P. 1968 *Deep Sea Res.* **15**, 267–274.



Downloaded from rsta.royalsocietypublishing.org

FIGURE 1. (a) Areas of detailed surveys on R.V. *Sarsia* in 1973, 1976, 1979 and 1980. The line of dots represents a series of STD stations completed in 1972. The shaded area represents the area covered by the synthetic aperture radar (s.a.r.) pass from SEASAT (see figure 9). The positions of shelf-break current meter moorings 001, 002 (see text and figure 13), 042, and 043 are also indicated. (b) Infrared image taken from NOAA-6 on 19th June 1979, showing cooling at the shelf break and the Ushant front. White represents low temperatures.

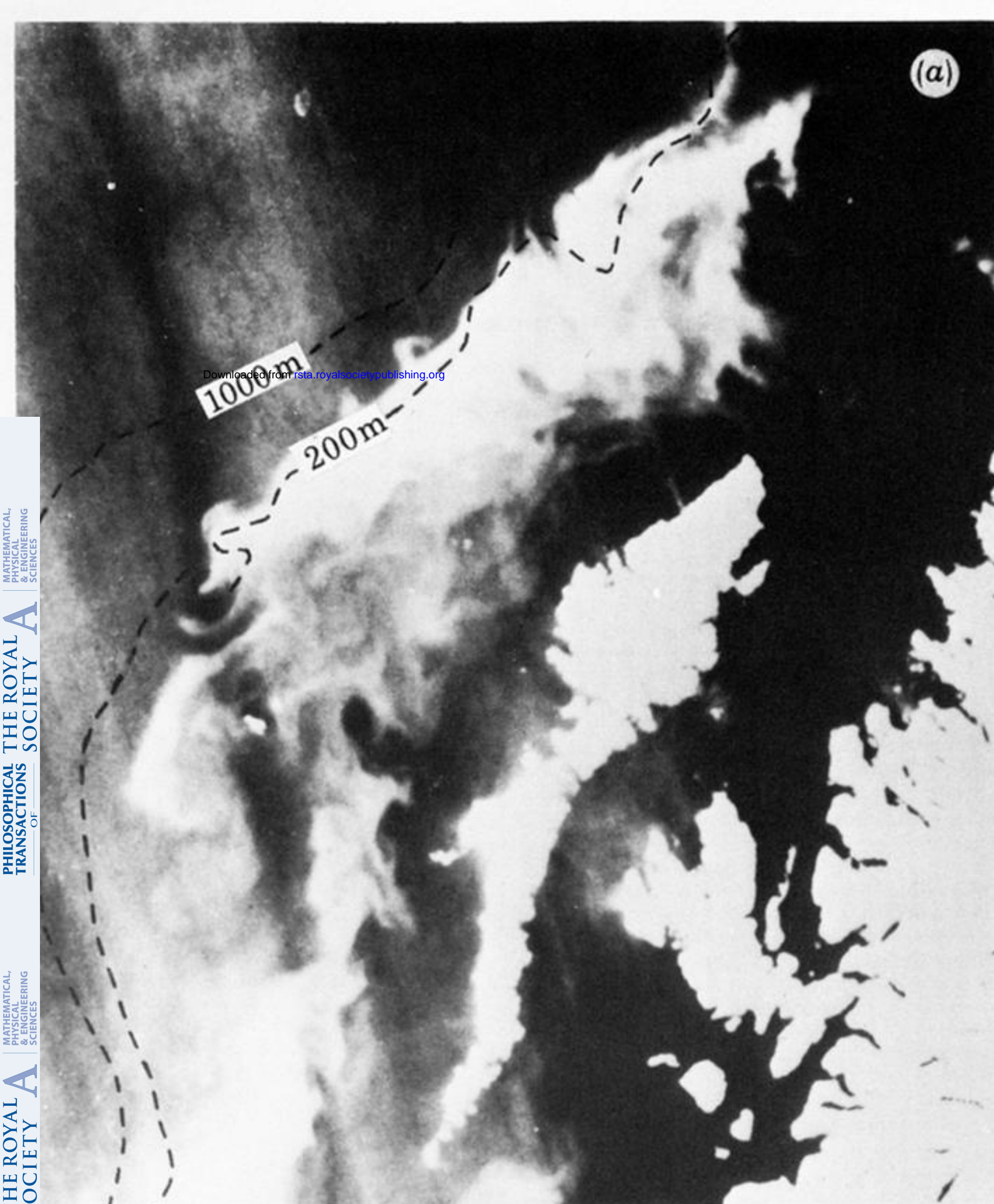


FIGURE 10. (a) Coastal zone colour scanner (c.z.c.s.) image (CH3) of the western (Hebrides) shelf break west of Scotland taken at 11h04 G.M.T. on 17 May 1980 from NIMBUS-7. The scanner is sensitive to chlorophyll or suspended sediments or both. White shading indicates increased chlorophyll in this region. (b) Infrared image of the same region taken from NOAA-6 on 17 May 1980 at 08h49 G.M.T.

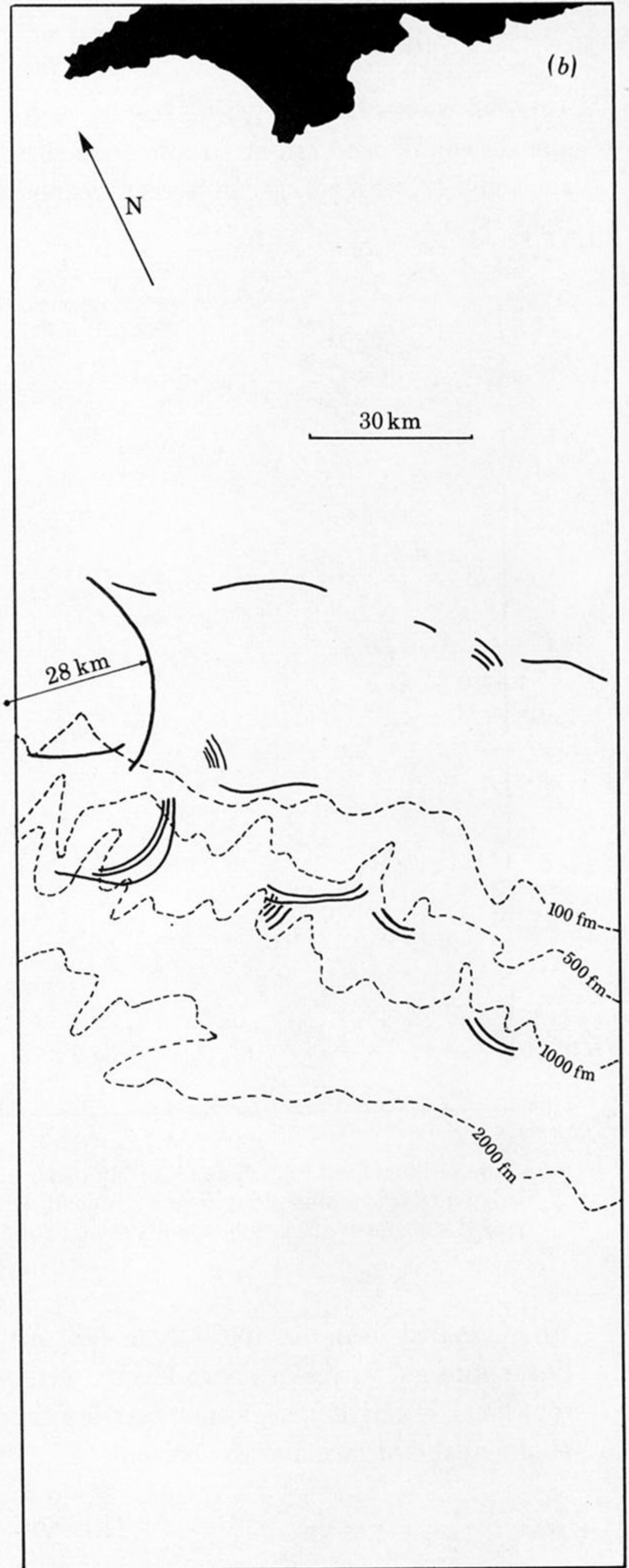
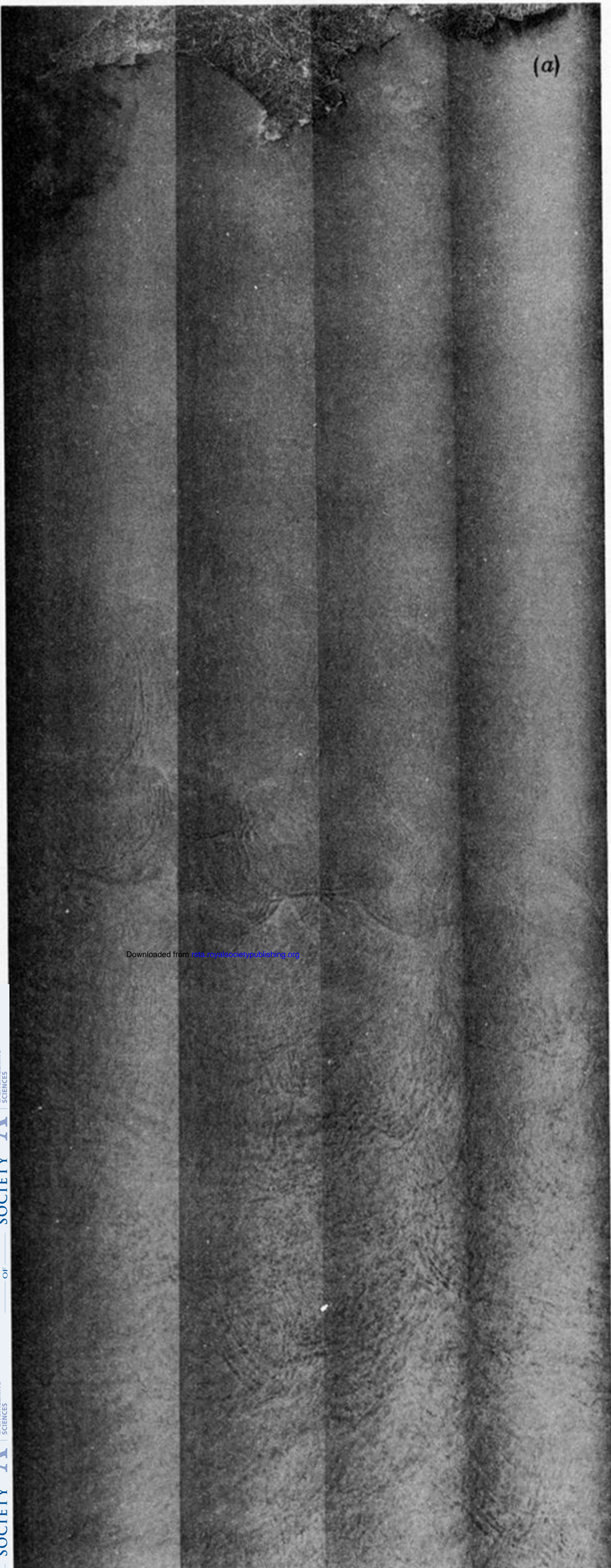


FIGURE 9. (a) Part of a synthetic aperture radar (s.a.r.) pass from SEASAT on 20 August 1978. For location see figure 1a. (b) Stylized pictures of the main features of interest in figure 9a. Depths are in fathoms (fm) owing to the use of chart C6568 (1 fm = 1.83 m).